IEEE Access
Multidisciplinary | Rapid Review | Open Access Journal

Received May 25, 2018, accepted June 24, 2018, date of publication June 29, 2018, date of current version July 19, 2018.

Digital Object Identifier 10.1109/ACCESS.2018.2851665

Active Vibration Suppression of Flexible Spacecraft During Attitude Maneuver With Actuator Dynamics

SHIJIE XU[1], NAIGANG CUI[2], YOUHUA FAN[1], AND YINGZI GUAN[2]
[1]Harbin Institute of Technology, Shenzhen 518055, China
[2]Harbin Institute of Technology, Harbin 150001, China

Corresponding author: Youhua Fan (yhfan@hit.edu.cn)

This work was supported by the National Natural Science Foundation of China under Grant 91648201.

ABSTRACT A novel active vibration suppression approach based on a flywheel actuator for flexible spacecraft during attitude maneuvering is proposed in this paper. The flywheel is regarded as the only actuator. The rotation of the flywheel, the motion of the rigid body, and the vibration of the modes are coupled in this paper. The system model is obtained using the Euler-Lagrange methodology and the Assumed-mode Method, in which the dynamics of the flywheel is considered. The stability of the flywheel transfer function from input voltage to output torque is analyzed using the Lyapunov method. Effects on system caused by flywheel are analyzed. Based on component synthesis vibration suppression theory, a typical vibration suppress law during attitude maneuver is derived. The input voltage of the flywheel actuator is designed according to this law. The presented novel approach is easily applied and practical without changing the spacecraft's structure properties. The simulation results and experiments on an air bearing spacecraft simulator are presented to verify the efficacy of the proposed approach.

INDEX TERMS Active vibration suppression, CSVS method, flexible spacecraft, reaction flywheel.

I. INTRODUCTION

To enable spacecraft to achieve sensitive and accurate attitude maneuvers, their mass and moment of inertia are reduced by a large margin, whereas the flexibility of the structures is increased. The vibration of flexible appendants will significantly affect pointing accuracy and slewing time. Thus, the suppression of flexible vibration is necessary [1]. In this study, active vibration suppression of flexible spacecraft by flywheel during attitude maneuvering will be investigated. A flywheel actuated single-axis gas suspending rotary table (SGSRT) with a flexible beam was used and modeled to be the simplified satellite.

For spacecraft with flexible appendants, strategies for vibration control during attitude maneuvering have been well-studied in the past [2]–[7]. C. Sendi and M. A. Ayoubi introduced a robust fuzzy controller for attitude stabilization of a rigid platform with a flexible appendage. The unavailable states were estimated by proposing a fuzzy observer [2]. This method improved the controller robust to parameter uncertainties and external disturbance. The optimal maneuver has also been studied extensively. J. Zheng, S. P. Banks and H. Alleyne extended the application of optimal control with linear quadratic regulator (LQR). They investigated the optimal control problem by approximating the coupled nonlinear system recursively to be a linear model and adopted LQR to stabilize the estimated linear flexible system [3]. Their contribution showed satisfactory results in attitude and vibration control. To ensuring the stability of spacecraft in the presence of external disturbance, Pukdeboon and Kumam [4] proposed a new robust optimal strategy to enhance the performance of existing sliding mode controller. This perfection was made by using an integral sliding mode control method. The control results in the presence of external disturbance illustrated the advantages of the works. S. Wu and S. Wen addressed a robust H-infinity output feedback control for attitude stabilization of flexible satellites. Furthermore, the convex optimization algorithm and a LMI-based output feedback controller are presented to deal with external disturbance and model uncertainties, respectively. This work has exhibited the superiority of H-infinity control method in attitude stabilization [5]. Flexible spacecraft attitude control is a synthetic problem related to system nonlinear, model uncertainty and external

disturbances. Strategies in other fields can also be referenced. J. Yao, Z. Jiao, and D. Ma proposed a nonlinear adaptive repetitive controller for an electrohydraulic servomechanism. Compared to traditional repetitive controllers, this proposed controller requires little exact knowledge of system parameters. Model uncertainty is one of the most common problems of flexible spacecraft. This controller may significative for the control of spacecraft [6]. J. Yao and W. Deng proposed an active disturbance rejection adaptive control strategy for motion control of hydraulic servo systems in the present of parametric uncertainties and unmodeled disturbances. It can be proofed that this method can eliminate the integration difficulties between parametric-adaptive-based and disturbance-observer-based controls. This work may also useful for the control of spacecraft in the present of parametric uncertainties [7]. Despite the advantages of these control schemes, the residual vibrations of flexible appendants have not been eliminated essentially. The residual vibration still exists and is regarded as a distraction.

To eliminate the residual vibrations, smart materials have been investigated and fabricated over the years. Smart materials, such as Shape Memory Alloys (SMAs), Magnetorheological material (MR), Electrorheological (ER) materials [8], Piezoelectric material (PM) [9], [10], can be used as both sensors and actuators in vibration suppression. Piezoelectric materials is one kind of the most used sensor and actuator because of its numerous advantages [11]. Many control and placement optimal strategies have been applied using smart materials [12]. For achieving active control of flexible structures, Wu *et al.* [13] presented a compensated positive position feedback strategy with piezoelectric actuators. Although the new proposed strategy improved the ability for frequency shift and spillover into lower order modes, the controlled modes needed to be well separated. To overcome the sensitive to modeling errors of controllers, Khushnood *et al.* [14] adopted the H-infinity control method with piezoelectric actuators for vibration suppression of a simplified flexible spacecraft. Vibration suppression is achieved effectively without causing spillover. However, vibration control was treated independent of attitude control. D. Chhabra, G. Bhushan, and P. Chandna studied the optimal placement of smart materials. A modified heuristic genetic algorithm was used as the optimization algorithm. As a result, the computational requirement was largely reduced [15]. Although smart materials have demonstrated many advantages, they change the structural properties of the flexible appendages via mechanical interference, which is clearly undesirable. This issue makes the application of smart materials for vibration suppression inappropriate from the engineering viewpoint.

The component synthesis vibration suppression (CSVS) method can suppress vibrations without additional structures attached on flexible structures. This method was first proposed by Liu *et al.* [16] for implementation of rendezvous and docking of flexible structures. Shan *et al.* [17] presented the CSVS method for vibration suppression of flexible structures using an air jet thruster and analyzed and improved the robustness of this method. Sharing a semblable principle, a vibration suppression method called input shaping was also widely used since its first appearance. Many control strategies have been proposed by combining one of these two methods with different control methods. Q. Hu and G. Ma integrated CSVS method and positive position feedback control for vibration control during attitude maneuver of flexible spacecraft. The CSVS method was mainly used to attenuate the vibrations caused by rapid maneuvers. Control strategies were used to active suppress the microvibrations after the slew [18]. Whereafter, they achieved the same aim by integrating CSVS method and sliding mode control [19]. The sliding mode control was used to accomplish asymptotic attitude maneuver commands while the CSVS method was used to modify the output commands. Although vibration suppression was achieved in the two studies, it is hard for thrusters to provide expected control torques. Then, Hu [20] presented a new approach for attitude maneuver and vibration suppression of flexible spacecraft. This approach combined input shaping method with robust nonlinear variable structure control strategy. Commands were modified by the input shaping method to get the expected status first. The robust controller was mainly for tracking the expected status and dealing with parametric uncertainty and external disturbances. In addition, compared with input shaping method, the CSVS method uses analytic methodology to get the commands, without solving nonlinear equations. Furthermore, the CSVS commands can be of many forms. Thus, the CSVS method become a practical vibration suppression technique.

Actuator plays an important role in vibration suppression of flexible appendants. A jet thruster has been widely used as its quick response and stability of output torque. Casella *et al.* [22] used jet thruster and piezoelectric as an actuator for attitude maneuvering and vibration suppression. However, a jet thruster is a life-time limited actuator which depends on the gas storage capacity of spacecraft. Moreover, smart materials are unable for the attitude maneuver of spacecraft. Devices able to generating continuous and precise torques without expending the propellant are needed [23]. Thus, the advantages of flywheels or control moment gyroscopes (CMGs) are highlighted [24], [25]. Shi and Damaren [26] considered a cantilevered beam as the research object and used CMGs and a collocated angular velocity sensor to damp the vibration. This work is easy to implement. However, the system in this study is specific. Although flywheels and CMGs have been used in maneuvering and vibration attenuation, few reports in the open literatures focused on the coupling of rotor electric circuit and flexible structures.

Motivated by the aforementioned survey, the major work and main contributions of this paper is summarized as follows. A single-link flexible manipulator coupled with a flywheel is modeled. The CSVS method is adopted in active vibration suppression of flexible appendants

during maneuvering. Effects on system caused by introducing of flywheel is analyzed via numerical calculation and experiment. Voltage schemes of flywheel for vibration suppression during attitude maneuver are designed according to CSVS method. The effectiveness of proposed approach is certified via practical simulations and experiments.

The remaining part of this paper is organized as follows. In section 2, a single-link flexible manipulator with a flywheel actuator is modeled. Section 3 presents the principle of CSVS method, and active vibration control schemes are designed. Moreover, the execution of the flywheel is analyzed. Section 4 illustrates the practical numerical simulations. Experimental works and the experimental results are discussed in section 5. Last, the study's conclusions are presented in section 6.

II. MATHEMATICAL MODEL

Fig. 1 shows the flexible manipulator system being modeled. This system consists of a rigid hub with radius b, a flexible beam and a flywheel. A single-link flexible manipulator is modeled as a uniform cantilever beam with the length l that rotates about the Z-axis perpendicular to the paper. A flywheel is fixed on the hub as an actuator. Control torque is provided by the flywheel along the Z-axis. Four assumptions are made first: (1) the beam is considered to be an Euler-Bernoulli beam, and axial deformation is neglected; (2) the gravitational effect and the hub dynamics are neglected for simplicity; (3) the flexible material of the beam is isotropic; and (4) the system is linear.

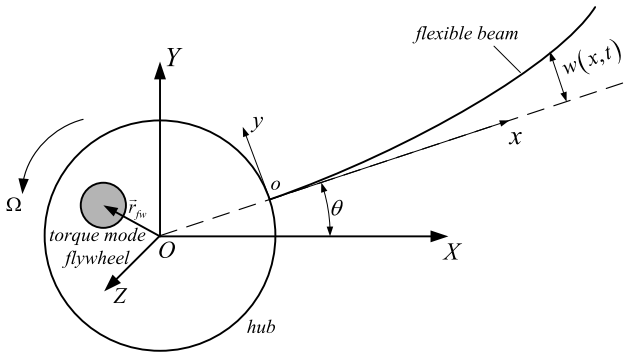

FIGURE 1. Diagram of the flexible manipulator.

Define $OXYZ$ and oxy as the inertial frame and the frame fixed on the edge of hub, respectively. $\theta(t)$ is the attitude angle of rigid hub. $w(x,t)$ is the flexible deformation at point x with respect to the oxy frame. $\boldsymbol{r}_{fw}$ is the vector from the origin of $OXYZ$ to the rotation center of flywheel. Ω is the angular velocity of rigid hub.

The modeling of this kind of system can be found in many existing literatures [27]. Furthermore, dynamics equations will be augmented to consider the effects of the flywheel. The equations will be obtained according to the Newton-Euler method and assumed mode method; the simplification of these equations representing attitude maneuvering and flexible vibration can be expressed as:

$$J\dot{\Omega} + J_w\dot{\Omega}_w + \boldsymbol{H}\ddot{\boldsymbol{\eta}} = T \tag{1}$$

$$J_w\dot{\Omega} + J_w\dot{\Omega}_w = Ik_T \tag{2}$$

$$\ddot{\boldsymbol{\eta}} + \boldsymbol{C}\dot{\boldsymbol{\eta}} + \boldsymbol{K}\boldsymbol{\eta} = -\boldsymbol{H}^{\boldsymbol{T}}\dot{\Omega} \tag{3}$$

where J represents the moment of inertia of rotation system, and J_w represents the moment of inertia of flywheel rotor. Ω_w is the angular velocity of flywheel. $\boldsymbol{H}$ denotes the coupling matrix between the flexible and rigid structure. $\boldsymbol{\eta}$ is the modal coordinate vector, and it is dimensionless. T is the external torque and disturbances. I denotes the current in flywheel and k_T is the motor torque constant. Furthermore, $\boldsymbol{C} = diag\{2\zeta_i\omega_{ni}, i = 1, 2, \ldots, N\}$ and $\boldsymbol{K} = diag\left\{\omega_{ni}^2, i = 1, 2, \ldots, N\right\}$ are the damping and stiffness matrix with the number of elastic modes considered N. ω_{ni} and ζ_i are the natural frequencies and corresponding damping, respectively.

In essence, the major part of flywheel is an electric motor; its dynamic equation is well known as

$$RI + L\dot{I} + k_e\Omega_w = U \tag{4}$$

where R, L, and k_e denotes armature resistance, armature inductance and back electromotive-force constant, respectively. U is the input voltage for electric motor.

Thus, the dynamics of flexible manipulator system can be expressed as

$$\begin{aligned} J\dot{\omega} + J_w\dot{\omega}_w + \boldsymbol{H}\ddot{\boldsymbol{\eta}} &= T \\ J_w\dot{\omega} + J_w\dot{\omega}_w &= Ik_T \\ \ddot{\boldsymbol{\eta}} + \boldsymbol{C}\dot{\boldsymbol{\eta}} + \boldsymbol{k}\boldsymbol{\eta} &= -\boldsymbol{H}^{\boldsymbol{T}}\dot{\omega} \\ RI + L\dot{I} + k_e\omega_w &= U \end{aligned} \tag{5}$$

In this paper, the vibration suppression of flexible manipulator during attitude maneuvering will be investigated using equation (5).

III. CSVS AND ACTIVE VIBRATION SUPPRESSION

In this section, a simple and effective method called the CSVS method will be introduced first. Next, the application of the CSVS method to suppress vibration is shown. Last, the CSVS method is applied on a flywheel command design for vibration suppression during flexible manipulator maneuvering. Furthermore, the stability of flywheel is analyzed.

A. CSVS THEORY

CSVS is an effective and simple technique to suppress the vibration actively during attitude maneuver. A typical component synthesis vibration suppression method is to divide one attitude control torque into two or more according to specified rules. After all the components are completed, the oscillations will cancel each other completely. Furthermore, vibrations generated during attitude maneuver can be suppressed in half natural period using the CSVS method. In this manner, there will be no residual vibration when maneuvering is completed. The basic principle of CSVS method is shown in Fig. 2.

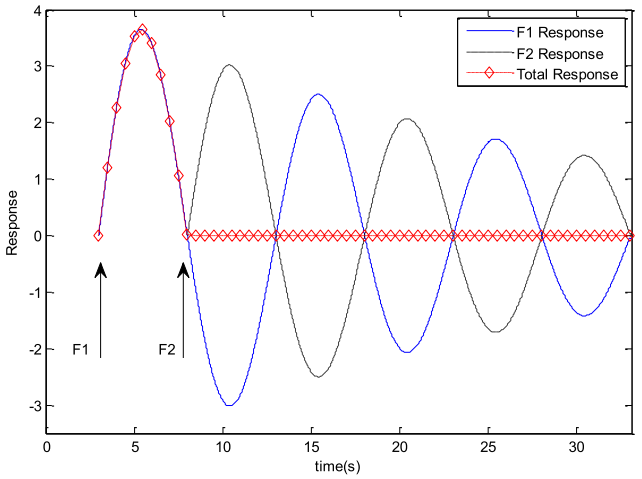

FIGURE 2. Basic principle of the CSVS method.

Assume there is a generalized vibration system that can be expressed as

$$\ddot{\eta}_i + 2\xi_i\omega_i\dot{\eta}_i + \omega_i^2\eta_i = F(t) \tag{6}$$

where η_i represents the vibration mode. Subscript i denotes the i-th vibration mode. ω_i is the i-th natural frequency. ξ_i is the i-th damp ratio. The system is excited by $F(t)$. To simplify the expression, the subscript i will be omitted henceforth.

As is shown in Fig. 2, excitation $F1$ is added at time instant t_0 and $F2$ is added at time instant t_1. Assume the magnitude of excitation $F1$ and $F2$ are A1 and A2, respectively. Solving (6), we have

$$\eta(t) = \frac{\omega}{\sqrt{1-\xi^2}} e^{-\xi\omega t} \begin{bmatrix} A_1 \sin(\omega_d (t-t_0)) \\ +A_2 e^{-\xi\omega t_1} \sin(\omega_d (t-t_1)) \end{bmatrix} \tag{7}$$

where $\omega_d = \omega\sqrt{1-\xi^2}$ is the damping natural frequency.

According to (7), if $F1$ and $F2$ are respectively added, we will have

$$\begin{cases} \eta_1(t) = \dfrac{A_1\omega}{\sqrt{1-\xi^2}} e^{-\xi\omega(t-t_0)} \sin(\omega_d (t-t_0)) \\ \eta_2(t) = \dfrac{A_2\omega}{\sqrt{1-\xi^2}} e^{-\xi\omega(t-t_1)} \sin(\omega_d (t-t_1)) \end{cases} \tag{8}$$

To ensure the residual vibration is zero after time instant t_1, the response after excitation $F2$ should be zero. Thus, solving (8), if $t_0 = 0$, we obtain

$$t_1 = \frac{m}{\omega\sqrt{1-\xi^2}} \quad m = 1, 2, \cdots \tag{9}$$

According to the CSVS principle, the component forces can be designed in an arbitrary time-varying form. Furthermore, the number of forces is unconstrained. This theory is also applicable and easier to prove when the damping is ignored. The system without damping can be expressed as

$$\ddot{\eta}_i + \omega_i^2\eta_i = Fc(t) \tag{10}$$

The symbols in (10) have the same definitions as those in (6).

Setting two time-varying forces $F1(t)$ and $F2(t)$, and their resultant force $Fc(t)$, $Fc(t)$ can be expressed as (11):

$$Fc(t) = \sum_{i=1}^{2} Fi(t) \tag{11}$$

The time-dependent laws of component forces $Fi(t)$ are the same as each other except for their starting time instant. Thus, (11) can be expressed as

$$Fc(t) = \sum_{i=1}^{n} f(t-t_i) * \delta(t-t_i); \quad n = 2 \tag{12}$$

where

$$\delta(t-t_i) = \begin{cases} 0, & t < t_i \\ 1, & t \geq t_i, \end{cases}$$
$$t_i = (i-1)\frac{2\pi}{n\omega} + \frac{2k\pi}{\omega}, \quad k = 0, 1, 2\cdots.$$

Function $f(t)$ illustrates an arbitrary time-dependent law. $\delta(t)$ is a time-delay function, and t_i denotes the delay time. Their curves and system responses generated by them are shown in Figs. 3-4.

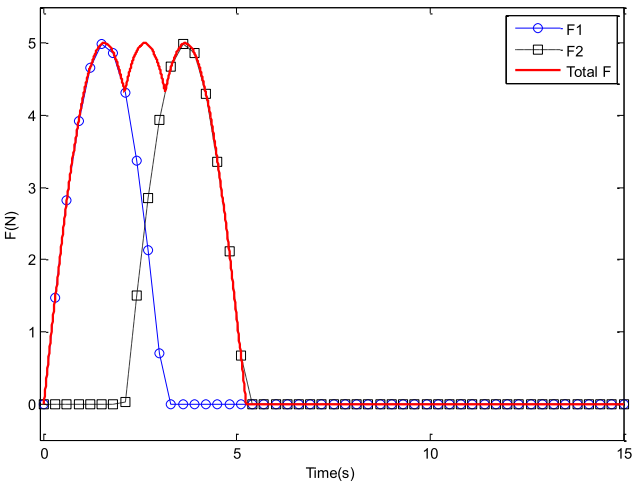

FIGURE 3. Component forces and resultant force.

According to the theory given in this section, there will be no residual vibration when all the component forces are finished. In the CSVS method, the frequencies of the system and the delay time of the component forces are important parameters that should receive great attention.

There are another three main theorems that extend the application of the CSVS method [17]. Those theorems can be applied to multimode vibration suppression by setting the suppress component forces of last order as the synthesis of next order. To simplify the process, damping will be ignored below.

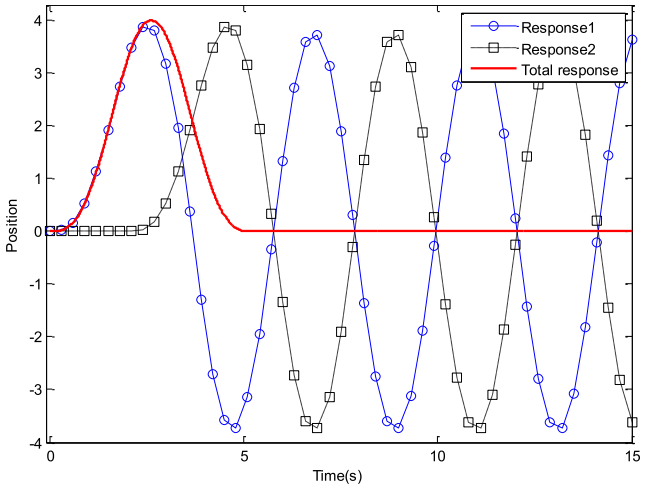

FIGURE 4. Responses of the component forces and the resultant force.

B. DESIGN OF THE VIBRATION SUPPRESSION SCHEME

The CSVS method can be regarded as a type of constraint. Control schemes can be properly designed in combination with this method. In this process, attitude maneuver will be realized without residual vibration. Generally, the first vibration mode contains the most energy of system vibration motion. The effect of suppression for the first vibration mode is the most representative. Thus, the scheme comprised of two component forces and mainly used for suppression of the first vibration mode according to the CSVS method will be designed. Another scheme without the CSVS method will also be considered for comparison. Assuming the first-order frequency of system is ω_1, its first vibration mode period can be expressed as $T_1 = 2\pi/\omega_1$. Thus, the control torque, either time-variant or time-invariant, is given as

$$T_{control} = \sum_{i}^{2} f_i (t - t_i)\, \delta (t - t_i) \tag{13}$$

where

$$\delta (t - t_i) = \begin{cases} 0, & t < t_i \\ 1, & t \geq t_i. \end{cases}$$

For time-invariant torque, we choose two steps to obtain component torque f_i, time-invariant component torque f_{t-inv} can be expressed as

$$f_{t-inv} = \begin{cases} A, & 0 < t < \alpha \\ -A, & \varphi < t < \varphi + \alpha \\ 0, & else \end{cases} \tag{14}$$

where A is the amplitude of steps, α is the duration of each step, and φ is the interval between the two start times of the steps.

For time-variant torque, f_i consists of the two time-variant function $g(t)$, time-variant component torque f_{t-var} can be expressed as

$$f_{t-var} = \begin{cases} g(t), & 0 < t < \alpha \\ -g(t), & \varphi < t < \varphi + \alpha \\ 0, & else \end{cases} \tag{15}$$

where $g(t)$ is a function with an arbitrary time-varying law.

According to the CSVS method, attitude maneuver control torques can suppress multi-order vibration modes by designing f_i. In this study, the first two vibration modes are considered. The interval between time instants of two component torques has a close relationship with the vibration suppression effects.

C. EXECUTION OF THE FLYWHEEL

The flywheel must be able to provide the same torque for the same input voltage command. From (4), we have the model of the flywheel. Next, we will discuss the stability of the flywheel.

According to (4), the block diagram of flywheel can be expressed in Fig. 5:

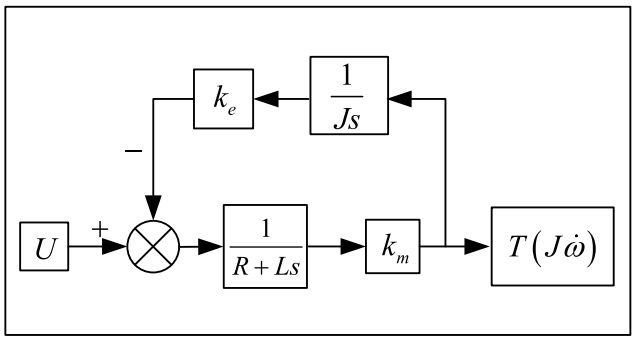

FIGURE 5. Block diagram for the flywheel.

The transfer function $G(s)$ of the flywheel is shown as:

$$G(s) = \frac{T}{U} = \frac{k_m J s}{Js(R + Ls) + k_e k_m} \tag{16}$$

Let the characteristic equation be 0; the characteristic roots can be calculated as

$$s_{1,2} = \frac{-JR \pm \sqrt{(JR)^2 - 4JLk_e k_m}}{2JL} \tag{17}$$

According to Lyapunov's first law, to ensure the system is stable, all of the characteristic roots should have a negative real part. In this situation, the flywheel is used as the actuator; thus, the characteristic roots must meet the condition. The stability of flywheel is dependent on its parameters.

IV. NUMERICAL SIMULATION

Numerical simulation is conducted to present the effectiveness of vibration suppression during attitude maneuvering by the flywheel. First, the parameters of model are given. Next, voltage commands with and without CSVS method will be given to the flywheel actuator to show the vibration suppression effective. Last, the responses are illustrated.

Numerical simulation is based on results obtained from our experiment facility, which shown in Fig. 9. The moment of inertia of the rigid hub is $J = 13$, and the moment of inertia of the flywheel rotor is $J_w = 0.042$. The coupled matrix of rotation and vibration is $\boldsymbol{H} = \begin{bmatrix} H_1 & H_2 \end{bmatrix} = \begin{bmatrix} 2.7641 & 0.6527 \end{bmatrix}$. All of these quantities are with the units of (kgm^2). The other main parameters of flywheel are shown in Table 1.

TABLE 1. Main parameters of motor.

Symbol	QUANTITY	Unit
k_T	motor torque constant	Nm/A
k_e	back electromotive-force constant	Vs/rad
L	armature inductance	H
R	armature resistance	Ω

Substituting the values of the parameters into (17), the flywheel can be proved to be stable. The first two elastic modes have been taken into account in the model used for simulation. Substituting those parameters into (5), the numerical model is confirmed. As is known, the first two vibration modes play a main role in the vibration motion. Thus, the other modes will be ignored here. The first and second natural frequencies of the system can be calculated: $\omega_1 = 2.8081$, $\omega_2 = 13.643$, with the units being (rad/s). The first and second damping are $\zeta_1 = \zeta_2 = 0.001$.

In numerical simulation, the single-link flexible manipulator will be considered as an ideal system, i.e., the initial state of the system and the external disturbances are assumed to be zero.

The vibration suppression schemes were previously discussed. For the flywheel actuator, the component voltage command is expressed as

$$f(t) = \begin{cases} 0, & 0 < t \le a \\ g(t-a), & a < t \le a+\tau \\ 0, & a+\tau < t \le b \\ -g(t-b), & b < t \le b+\tau \\ 0, & t > b+\tau \end{cases} \tag{18}$$

where $g(t)$ is an arbitrary function of time; here, we set $g(t) = 6$ V. a and b are two time instants of the voltage command. τ is the duration of the commands. The final voltage command, U, consists of two component voltage commands and can be expressed as

$$\begin{bmatrix} U(t) \\ t \end{bmatrix} = \begin{bmatrix} f(t-t_1) & f(t-t_2) \\ 0 & \left(n+\frac{1}{2}\right)\frac{2\pi}{\omega_1} \end{bmatrix} \quad n = 0, 1, 2, \cdots \tag{19}$$

As is demonstrated in the CSVS method, time instants a and b should have the following relationship:

$$b - a = m\frac{2\pi}{\omega_1} \quad m = 1, 2, \cdots \tag{20}$$

The suppression of the first vibration mode is taken as representative. The methods of suppressing multi-order natural vibration modes share the same principle and will not be discussed here.

The duration and interval times between two commands should be receive considerable attention. For most feedback control methods, the interval time between commands depends on their controller, and its value is arbitrary. Those types of commands always cause obvious residual vibration. Commands without the CSVS method will be applied to represent commands from feedback controllers and used for comparison. Both of the methods share a same characteristic, namely, the interval times between two commands are arbitrary. In contrast, the interval times in the command with CSVS method are controlled strictly. The results of the two types of commands are shown in Figs. 6-8.

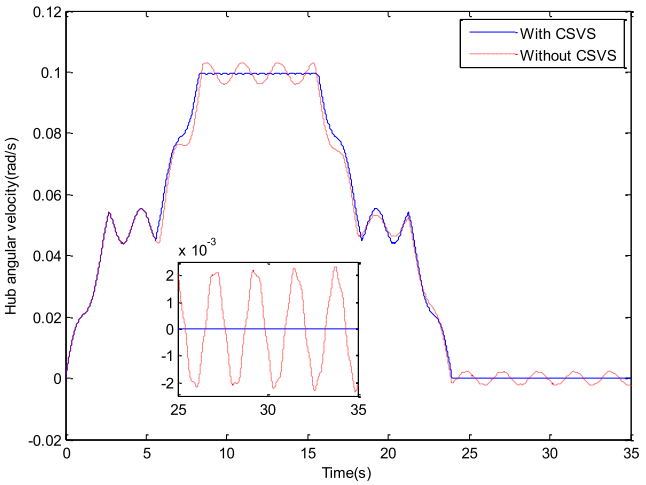

FIGURE 6. Hub angular velocity under two commands.

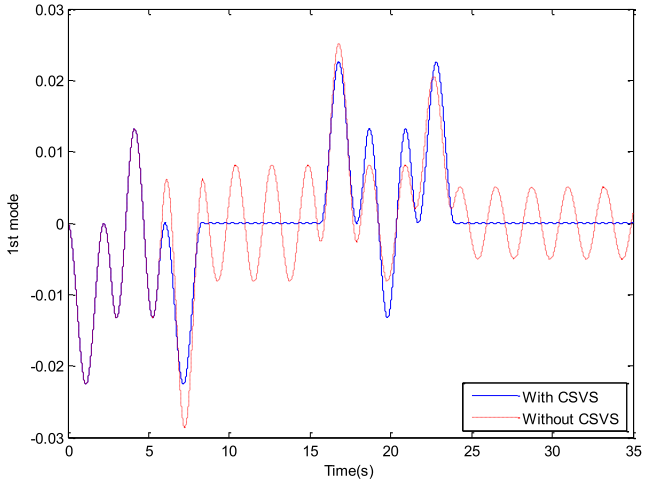

FIGURE 7. First vibration mode under two commands.

Hub angular velocity has two types of processes, as shown in Fig. 6. The first process is during attitude maneuvering, when the angular velocity changes significantly. The second

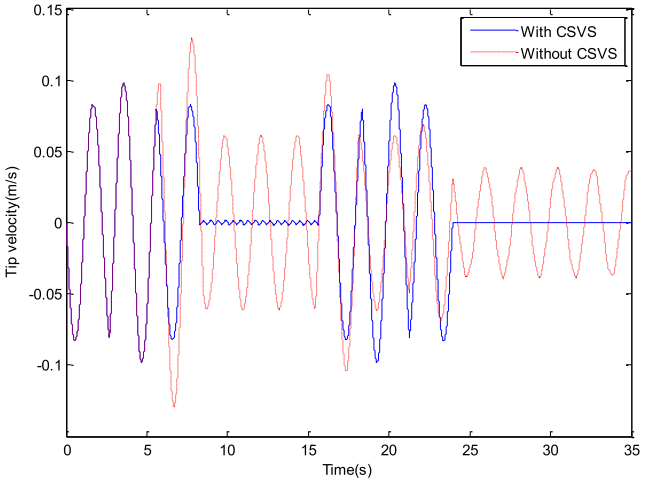

FIGURE 8. Tip velocity under two commands.

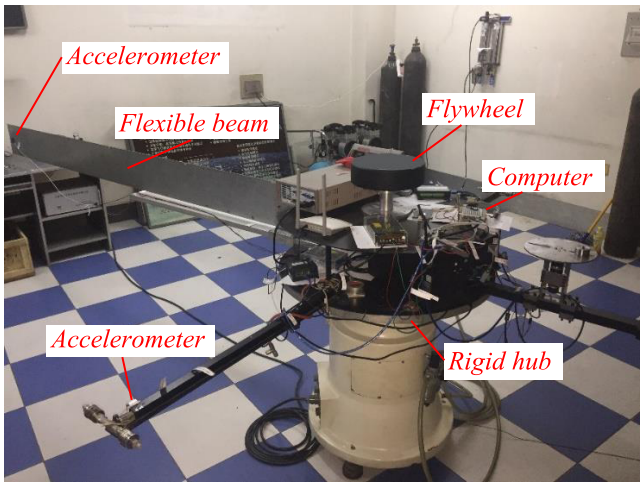

FIGURE 9. Experimental setup of a single-axis rotary table.

process is from the time instant that the command is finished, when the variation becomes stable. Enlarger shows the difference of two results in the second process. Focusing on the second process, the result from the command without CSVS method has amplitude that is considerably higher than that from the command with the CSVS method. Chattering of the results from the command with the CSVS method is negligible.

The data in Fig. 7 are similar to the data in Fig. 8 because the first vibration mode plays the main role in the structure vibration motion. Take the data shown in Fig. 8 as an example, two types of processes are observed. Tip velocity is chattering during the time when the voltage command is active. Differences between two command laws lead to minor differences in responses, such as the curves during 16-24 s. We find that the motion becomes stable when the voltage command is finished. Compared with the result under command without CSVS method, the CSVS method caused the tip velocity chatter to be much smaller. There is almost no energy in the first vibration mode, as shown in Fig. 7.

V. EXPERIMENTAL RESULTS

Experiments were further performed on an SGSRT actuated by a flywheel to validate the vibration suppression. SGSRT with correlative facilities are shown in Fig. 9.

The setup mainly consists of a rigid hub, a flexible aluminum beam (2480 mm $\times$ 200 mm $\times$ 2.5 mm), a torque mode flywheel (max torque is 0.06 Nm), and a number of measuring and data reception instruments. The rotary table is suspended by a gas bearing. The zero gravity environment is simulated, and the table is limited to rotate on the horizontal plane. The vibration of the flexible beam is measured by two accelerometers. The model of the accelerometer is 2220-020 produced by Silicon Design Inc. One accelerometer is fixed on the tip of flexible beam for monitoring the motion of beam, and another is fixed on the edge of hub for monitoring the accelerated velocity of the hub. The rotational speed of the hub is also measured by a TL632D-MEMS gyroscope that is placed on the hub. The system is acted by a flywheel.

To identify the main characteristics of the experiment system, free vibration tests were first performed. In those tests, the system motion was initiated by a pulsed excitation. Next, the tip acceleration was measured by the accelerometer. Fast Fourier transform (FFT) was implemented to determine the characteristics in the frequency domain. Fig. 10 demonstrates the measured acceleration data and the FFT result.

The measurement range of the accelerometers is ± 2 g and 0-400 Hz. High-frequency interference sources, such as the air compressor, the door of the laboratory, and people walking around, will cause the measured data to be complex. Thus, a low-pass filter with passband frequency of 0.314-30 rad/s is applied to the measured data. This filter is a function integrated in "SPTOOL" toolbox of Matlab. The results illustrated the first and second vibration modes play a main role, especially the first mode. The measured frequencies of first and second modes are 2.7382 rad/s and 13.9487 rad/s, respectively. The frequencies, measured and calculated, of the first two modes are shown in Table 2.

TABLE 2. First and second mode frequencies.

	1ST MODE FREQUENCY(RAD/S)	2ND MODE FREQUENCY(RAD/S)
Measured	2.7382	13.9487
Calculated	2.8081	13.643
Error	2.781%	2.19%

The errors are 2.781% and 2.19% for the first and second modes, respectively. It is inescapable and acceptable for the errors to arise between the mathematical model and the experimental equipment measurements. The measured frequencies will be used in the voltage command design.

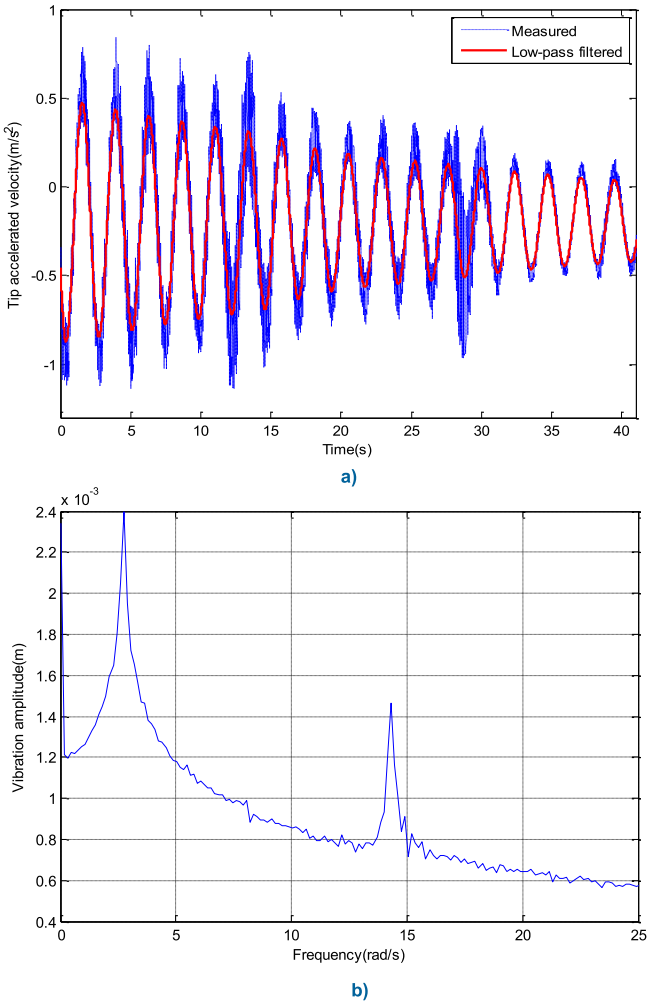

FIGURE 10. Tip free vibration and FFT analysis. a) Measured and filtered tip free vibration. b) FFT of tip free vibration.

A step voltage command is used in this experiment. Two voltage commands with the CSVS law will be adopted in our experiment to verify the effectiveness of vibration suppression during attitude maneuvering. The voltage commands U_a and U_b are shown in (21) and (22), respectively:

$$\begin{bmatrix} U_a \\ t_a \end{bmatrix} = \begin{bmatrix} 0 & 12 & 0 & -12 & 0 \\ 0 & 38 & 43.73 & 51.74 & 57.47 \end{bmatrix} \tag{21}$$

$$\begin{bmatrix} U_b \\ t_b \end{bmatrix} = \begin{bmatrix} 0 & 12 & 0 & 12 & 0 & -12 & 0 & -12 & 0 \\ 0 & 31 & 35.58 & 41.31 & 45.89 & 53.9 & 58.48 & 64.2 & 68.79 \end{bmatrix} \tag{22}$$

where U and t are of the units of (V) and (s), respectively.

The flitted measured results are plotted in Figs. 11-16. Figs. 11-13 show three key parameters in experiment A. The results demonstrated in Figs. 14-16 are the key parameters in experiment B.

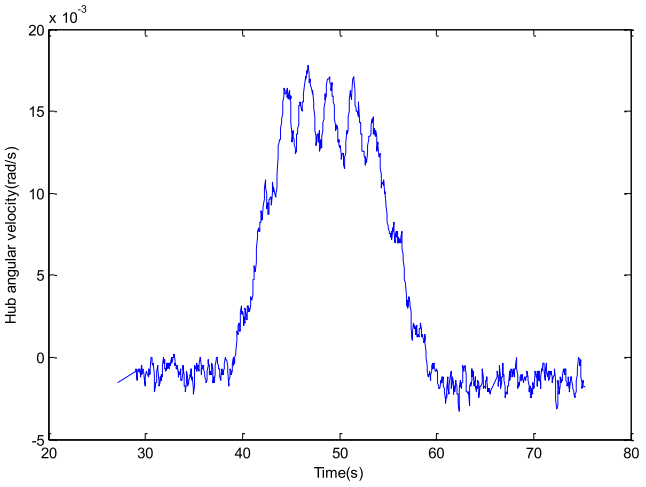

FIGURE 11. Hub angular velocity in experiment A.

Fig. 11 shows the hub angular velocity history in experiment A. The results reveal that the hub velocity changes substantially during 38-44 s and 52-58 s when the control torque is acting. The hub velocity is chattering notably between the time instants 44 s and 52 s. The motion status after 58 s is almost the same as the status before 38 s. Beam vibration causing the initial charting is impossible to completely eliminate in the experiments. Moreover, it is extremely difficult to ensure the center of mass of the SGSRT remains on the rotation axis; thus, the initial hub velocity is not equal to zero.

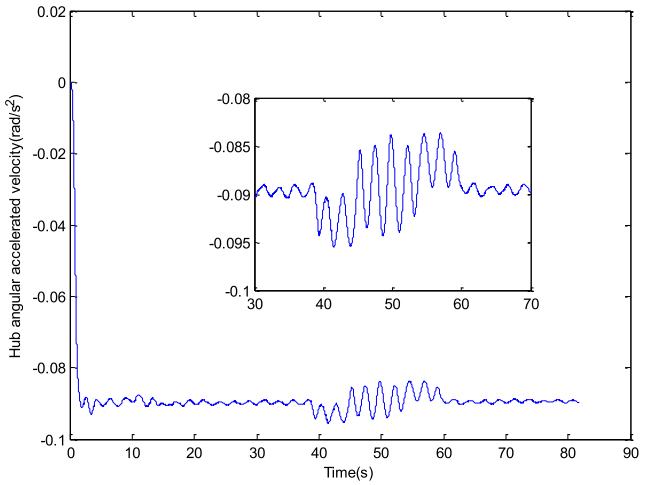

FIGURE 12. Hub angular accelerated velocity in experiment A.

Figs. 12-13 present the filtered data measured by accelerometers fixed on the edge of rigid hub, with one being located 1.04 m to the hub rotation axis and the other being at the tip of flexible beam in experiment A. The two figures show the same variation tendency. According to the measured information, the table system vibrated intensely from instant 38 s to 58 s. Compared with the initial state, the vibration energy after 58 s was not enhanced. There is

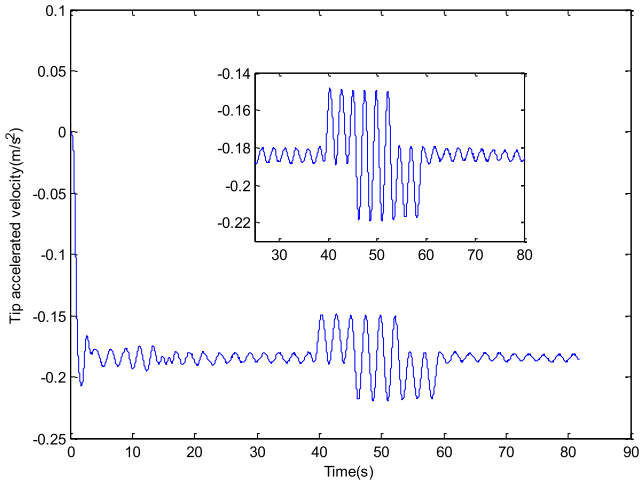

FIGURE 13. Tip accelerated velocity in experiment A.

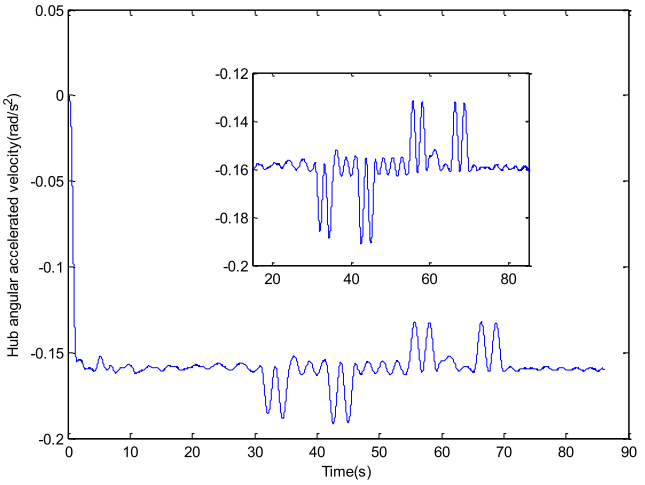

FIGURE 15. Hub angular accelerated velocity in experiment B.

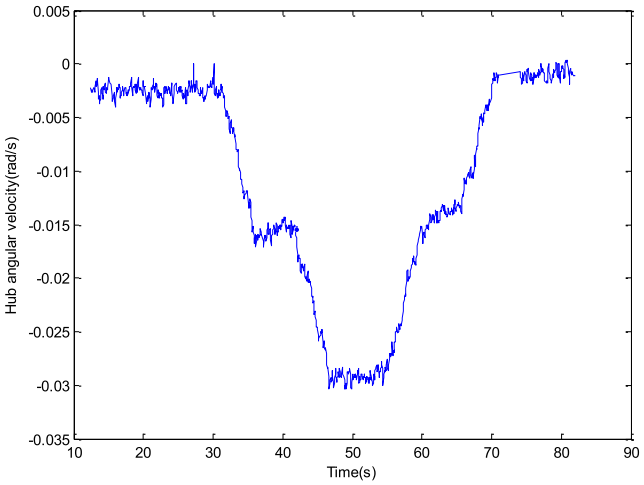

FIGURE 14. Hub angular velocity in experiment B.

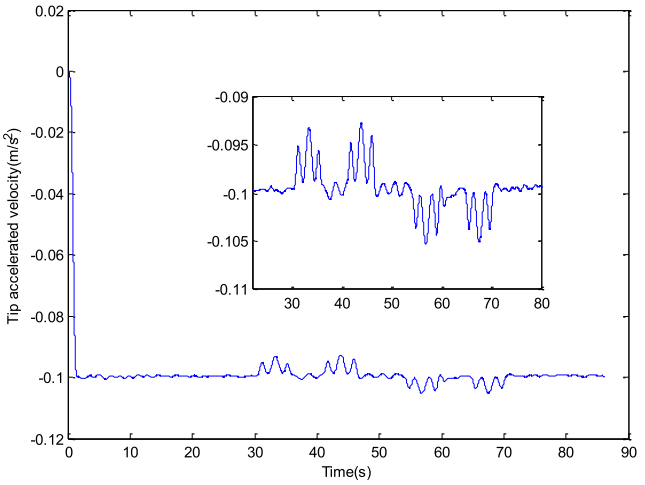

FIGURE 16. Tip accelerated velocity in experiment A.

almost no difference between two stages before and after the control torques. The vibration of beam has a deep relationship with the chattering of the hub.

Another experiment is performed to verify the effect of control scheme. Control torque B, expressed in (21), in experiment B is more complex than that in experiment A.

Fig. 14 demonstrates the hub angular velocity history in experiment B. Unlike experiment A, the vibration energy between two step torques remains the same as its initial state. Although the control torques become more complex, the stable rotation velocity after maneuvering oscillation is not greater than that in the initial stage.

Figs. 15 and 16 illustrate the accelerated velocity history of edge of the hub and tip of the flexible beam, respectively. The two states are chattering significantly during the maneuver process from 31 s to 69 s. The stable performances of the two accelerated velocity are the same as the performances before 31 s. The vibration amplitude after 69 s is not greater than that before 31 s. Both of these results verify the effectiveness of proposed scheme. It is particularly evident that the vibration energy is not enhanced after the maneuver torque.

VI. CONCLUSIONS

This paper presented an investigation of an active vibration suppression approach based on a flywheel actuator for flexible spacecraft during attitude maneuver. Flexible spacecraft coupled with flywheel dynamics is modeled. The transfer function of the flywheel is verified to be stable from input voltage to output torque. It is proved that the flywheel can output the expected control torques efficiently. Furthermore, numerical calculations and experiments demonstrate that the introducing of flywheel will not change the frequencies of system. To suppress vibrations during attitude maneuvering by the flywheel, the input voltage is designed in detail according to the CSVS method. The practical simulations and experiment results illustrate the effectiveness of proposed

approach. Investigations about the vibration suppression in the presence of inertia uncertainty and external disturbances will be considered in the future.

REFERENCES

[1] N. Ji and J. Liu, "Vibration control for a flexible satellite with input constraint based on Nussbaum function via backstepping method," *Aerosp. Sci. Technol.*, vol. 77, pp. 563–572, Jun. 2018.
[2] C. Sendi and M. A. Ayoubi, "Robust fuzzy logic-based tracking control of a flexible spacecraft with H_∞ performance criteria," in *Proc. AIAA Space Conf.*, San Diego, CA, USA, 2014, pp. 133–145.
[3] J. Zheng, S. P. Banks, and H. Alleyne, "Optimal attitude control for three-axis stabilized flexible spacecraft," *Acta Astronaut.*, vol. 56, no. 5, pp. 519–528, Mar. 2005.
[4] C. Pukdeboon and P. Kumam, "Robust optimal sliding mode control for spacecraft position and attitude maneuvers," *Aerosp. Sci. Technol.*, vol. 43, pp. 329–342, Jun. 2015.
[5] S. Wu and S. Wen, "Robust H_∞ output feedback control for attitude stabilization of a flexible spacecraft," *Nonlinear Dyn.*, vol. 84, no. 1, pp. 405–412, Apr. 2016.
[6] J. Yao, Z. Jiao, and D. Ma, "A practical nonlinear adaptive control of hydraulic servomechanisms with periodic-like disturbances," *IEEE/ASME Trans. Mechatronics*, vol. 20, no. 6, pp. 2752–2760, Dec. 2015.
[7] J. Yao and W. Deng, "Active disturbance rejection adaptive control of hydraulic servo systems," *IEEE Trans. Ind. Electron.*, vol. 64, no. 10, pp. 8023–8032, Oct. 2017.
[8] M. Azadi, S. A. Fazelzadeh, M. Eghtesad, and E. Azadi, "Vibration suppression and adaptive-robust control of a smart flexible satellite with three axes maneuvering," *Acta Astronaut.*, vol. 69, nos. 5–6, pp. 307–322, Sep. 2011.
[9] Z. Zhang, J. Kan, S. Wang, H. Wang, C. Yang, and S. Chen, "Performance dependence on initial free-end levitation of a magnetically levitated piezoelectric vibration energy harvester with a composite cantilever beam," *IEEE Access*, vol. 5, pp. 27563–27572, Nov. 2017.
[10] D. Xu, Y. Liu, J. Liu, S. Shi, and W. Chen, "Motion planning of a stepping-wriggle type piezoelectric actuator operating in bending modes," *IEEE Access*, vol. 4, pp. 2371–2378, May 2016.
[11] V. Sethi, M. Franchek, and G. Song, "Active multimodal vibration suppression of a flexible structure with piezoceramic sensor and actuator by using loop shaping," *J. Vib. Control*, vol. 17, no. 13, pp. 1994–2006, Jan. 2011.
[12] M. A. Khushnood, X. Wang, and N. Cui, "A criterion for optimal sensor placement for minimizing spillover effects on optimal controllers," *J. Vib. Control*, vol. 24, no. 8, pp. 1469–1487, Jul. 2016.
[13] Y. Wu, W. Zhang, X. Meng, and Y. Su, "Compensated positive position feedback for active control of piezoelectric structures," *J. Intell. Mater. Syst. Struct.*, vol. 29, no. 3, pp. 397–410, May 2017.
[14] M. A. Khushnood, X. Wang, and N. Cui, "Active vibration control of a slewing spacecraft's panel using H_∞ control," *J. Vibroeng.*, vol. 18, no. 5, pp. 2959–2973, Apr. 2016.
[15] D. Chhabra, G. Bhushan, and P. Chandna, "Optimal placement of piezoelectric actuators on plate structures for active vibration control via modified control matrix and singular value decomposition approach using modified heuristic genetic algorithm," *Mech. Adv. Mater. Struct.*, vol. 23, no. 3, pp. 272–280, Oct. 2015.
[16] D. Liu, D. Yang, and W. Zhang, "An optimal maneuver control method for the spacecraft with flexible appendages," in *Proc. Astrodyn. Conf.*, Minneapolis, MN, USA, 1988, pp. 294–300.
[17] J. Shan, D. Sun, and D. Liu, "Design for robust component synthesis vibration suppression of flexible structures with on-off actuators," *IEEE Trans. Robot. Autom.*, vol. 20, no. 3, pp. 512–525, Jun. 2004.
[18] Q. Hu and G. Ma, "Vibration suppression of flexible spacecraft during attitude maneuvers" *J. Guid. Control Dyn.*, vol. 28, no. 2, pp. 377–380, Mar. 2005.
[19] Q.-L. Hu and G.-F. Ma, "Flexible spacecraft vibration suppression using PWPF modulated input component command and sliding mode control," *Asian J. Control*, vol. 9, no. 1, pp. 20–29, Mar. 2007.
[20] Q. Hu, "Input shaping and variable structure control for simultaneous precision positioning and vibration reduction of flexible spacecraft with saturation compensation," *J. Sound Vib.*, vol. 318, nos. 1–2, pp. 18–35, Nov. 2008.
[21] X. Cao, C. Yue, and M. Liu, "Flexible satellite attitude maneuver via constrained torque distribution and active vibration suppression," *Aerosp. Sci. Technol.*, vol. 67, pp. 387–397, Aug. 2017.
[22] F. Casella, A. Locatelli, and N. Schiavoni, "Modeling and control for vibration suppression in a large flexible structure with jet thrusters and piezoactuators," *IEEE Trans. Control Syst. Technol.*, vol. 10, no. 4, pp. 589–599, Jul. 2002.
[23] Q. Hu, Y. Jia, and S. Xu, "Adaptive suppression of linear structural vibration using control moment gyroscopes," *J. Guid. Control Dyn.*, vol. 37, no. 3, pp. 990–996, May 2014.
[24] Y. Zhang, M. Li, and J. Zhang, "Vibration control for rapid attitude stabilization of spacecraft," *IEEE Trans. Aerosp. Electron. Syst.*, vol. 53, no. 3, pp. 1308–1320, Jun. 2017.
[25] Z. Yao, Z. Jingrui, and X. Shijie, "Parameters design of vibration isolation platform for control moment gyroscopes," *Acta Astron.*, vol. 81, no. 2, pp. 645–659, Dec. 2012.
[26] J.-F. Shi and C. J. Damaren, "Control law for active structural damping using a control moment gyro," *J. Guid. Control Dyn.*, vol. 28, no. 3, pp. 550–553, May 2012.
[27] S. D. Gennaro, "Output stabilization of flexible spacecraft with active vibration suppression," *IEEE Trans. Aerosp. Electron. Syst.*, vol. 39, no. 3, pp. 747–759, Jul. 2003.

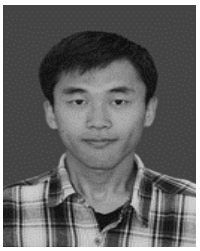

SHIJIE XU received the B.S. degree in engineering mechanics from Harbin Engineering University, Harbin, Hei Longjiang, China, in 2011, and the M.S. degree in mechanics from the Harbin Institute of Technology, Shenzhen, Guangdong, China, in 2013, where he is currently pursuing the Ph.D. degree in mechanics.

From 2013 to 2016, he was an Assistant Teacher with the Department of Aerospace Engineering, Harbin Institute of Technology, Harbin. His research interest includes the dynamic analysis of large flexible system and vibration suppression and control.

Mr. Xu is a member of the American Society of Mechanical Engineers. He was a recipient of the ISPS Division Graduate Student Scholarship in 2016.

NAIGANG CUI received the B.S. degree in vehicle system engineering from the National University of Defense Technology, Changsha, Hunan, China, in 1986, and the M.S. degree in flight mechanics and the Ph.D. degree in guidance and control and simulation from the Harbin Institute of Technology, Harbin, Hei Longjiang, China, in 1989 and1996, respectively.

He has been a Professor with the School of Astronautics, Harbin Institute of Technology, since 2000. His research interest includes flight mechanics and control of spacecraft, filtering theory and application, and spacecraft dynamics and control.

Dr. Cui is a Committee Member of the China Space Institute of Aerodynamics and the Flight Mechanics of Specialized Committee.

YOUHUA FAN received the B.S. degree in nuclear physics from the University of South China, Hengyang, Hunan, China, in 1996, and the M.S. degree in flight vehicle design and the Ph.D. degree in general and fundamental mechanics from the Harbin Institute of Technology, Harbin, Hei Longjiang, China, in 1998 and 2001.

He has been a Professor with the Harbin Institute of Technology, Shenzhen, since 2010. He has authored over 50 research papers. His research interest includes elastodynamics and its application and structural dynamics and applications.

Dr. Fan is a Lifetime Member of the China Geophysical Society and the Committee of Heilongjiang Industrial and Applied Mathematics Society.

YINGZI GUAN received the B.S. and M.S. degrees in mechanical design and manufacturing from the Nanjing University of Science and Technology, Nanjing, Jiangsu, China, in 1990 and 1993, respectively, and the Ph.D. degree in flight vehicle design from the Harbin Institute of Technology, Harbin, Hei Longjiang, China, in 2000.

She has been a Professor with the School of Astronautics, Harbin Institute of Technology Since 2008. She has authored over 30 research papers. Her research interest includes modeling and simulation of spacecraft dynamics.

Dr. Guan is a committee of space electronics and space optics specialized committee of the Chinese Society of Space Science.